On the Exploitation of Non-Radiating Currents to Design Geometry-Constrained Reflectarray Antennas

M. Salucci, A. Gelmini, G. Oliveri, N. Anselmi, and A. Massa

Abstract

In this work, the design of reflectarray surface currents able to meet both radiation and arbitrary geometry constraints is dealt with. Towards this goal, the synthesis problem is formulated as an inverse source one, and a closed-form expression solution is derived to compute the non-radiating current components able to modify the geometry of the reflective surface without altering the desired radiation features. Some representative numerical benchmarks are shown to assess the proposed synthesis methodology, as well as to verify its flexibility in realizing "*forbidden-regions*" of arbitrary shape.

Contents

1 Numerical Results

1.1 Shape - "O LCD-Like @ Center"

Parameters

- Number of reflectarray elements: $M = 81$, $N = 69$;
- Operative frequency: $f = 3.6$ [GHz];
- Polarization: L-CO;
- Number of elements in the forbidden region: $Q = 32$;

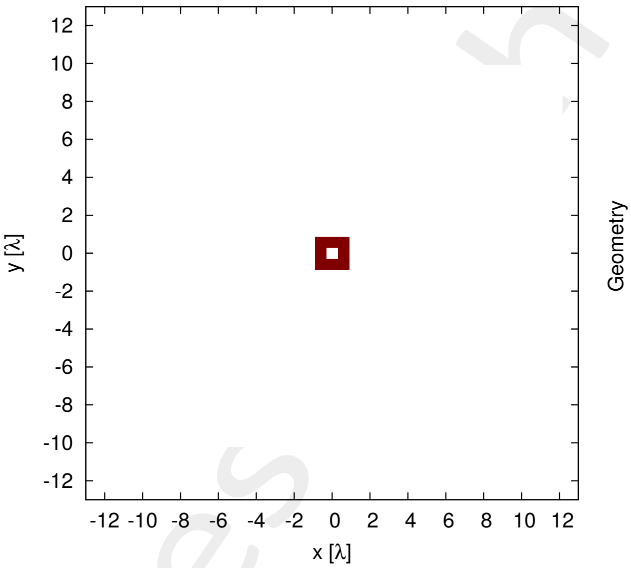

Figure 1: Geometry of forbidden region Ω.

Results

Magnitude and phase of the *NR* coefficients.

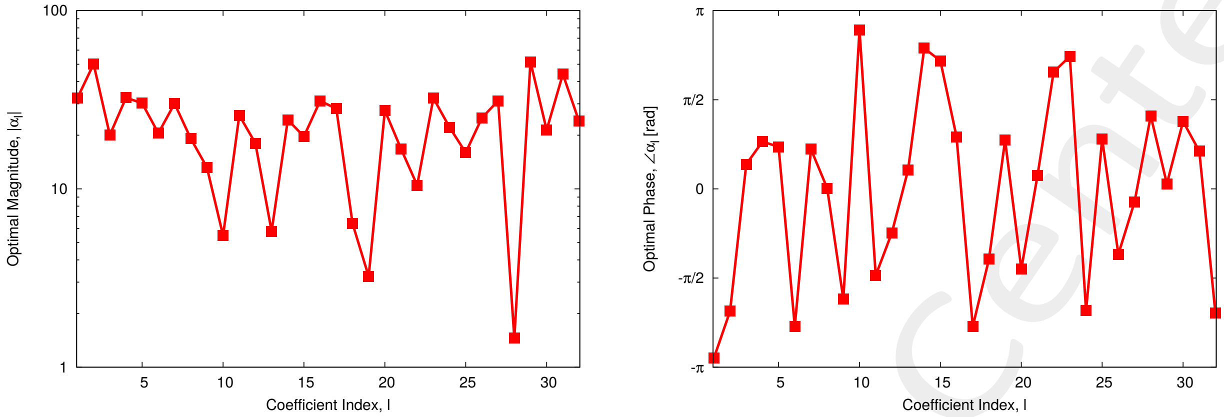

(a) (b)

Figure 2: Magnitude (a) and phase (b) of the solution.

Index q	$\Re\{\alpha_q\}$	$\Im\{\alpha_q\}$	Index q	$\Re\{\alpha_q\}$	$\Im\{\alpha_q\}$	Index q	$\Re\{\alpha_q\}$	$\Im\{\alpha_q\}$
1	-3.20×10^{1}	-5.25	12	1.29×10^{1}	-1.26×10^{1}	23	-2.23×10^{1}	2.34×10^{1}
2	-2.77×10^{1}	-4.19×10^{1}	13	5.48	1.88	24	-1.20×10^{1}	-1.86×10^{1}
3	1.82×10^{1}	8.42	14	-1.92×10^{1}	1.50×10^{1}	25	1.02×10^{1}	1.23×10^{1}
4	2.19×10^{1}	2.40×10^{1}	15	-1.25×10^{1}	1.52×10^{1}	26	1.02×10^{1}	-2.29×10^{1}
5	2.23×10^{1}	2.04×10^{1}	16	1.90×10^{1}	2.47×10^{1}	27	3.04×10^{1}	-7.08
6	-1.55×10^{1}	-1.35×10^{1}	17	-2.12×10^{1}	-1.85×10^{1}	28	4.07×10^{-1}	1.40
7	2.31×10^{1}	1.94×10^{1}	18	2.10	-6.04	29	5.14×10^{1}	4.58
8	1.92×10^{1}	2.04×10^{-1}	19	2.11	2.44	30	7.99	1.98×10^{1}
9	-4.75	-1.23×10^{1}	20	4.31	-2.72×10^{1}	31	3.47×10^{1}	2.72×10^{1}
10	-5.15	1.85	21	1.63×10^{1}	3.91	32	-1.39×10^{1}	-1.95×10^{1}
11	1.18	-2.58×10^{1}	22	-4.94	9.25			

Table I: Solution of the linear system

Currents Distribution

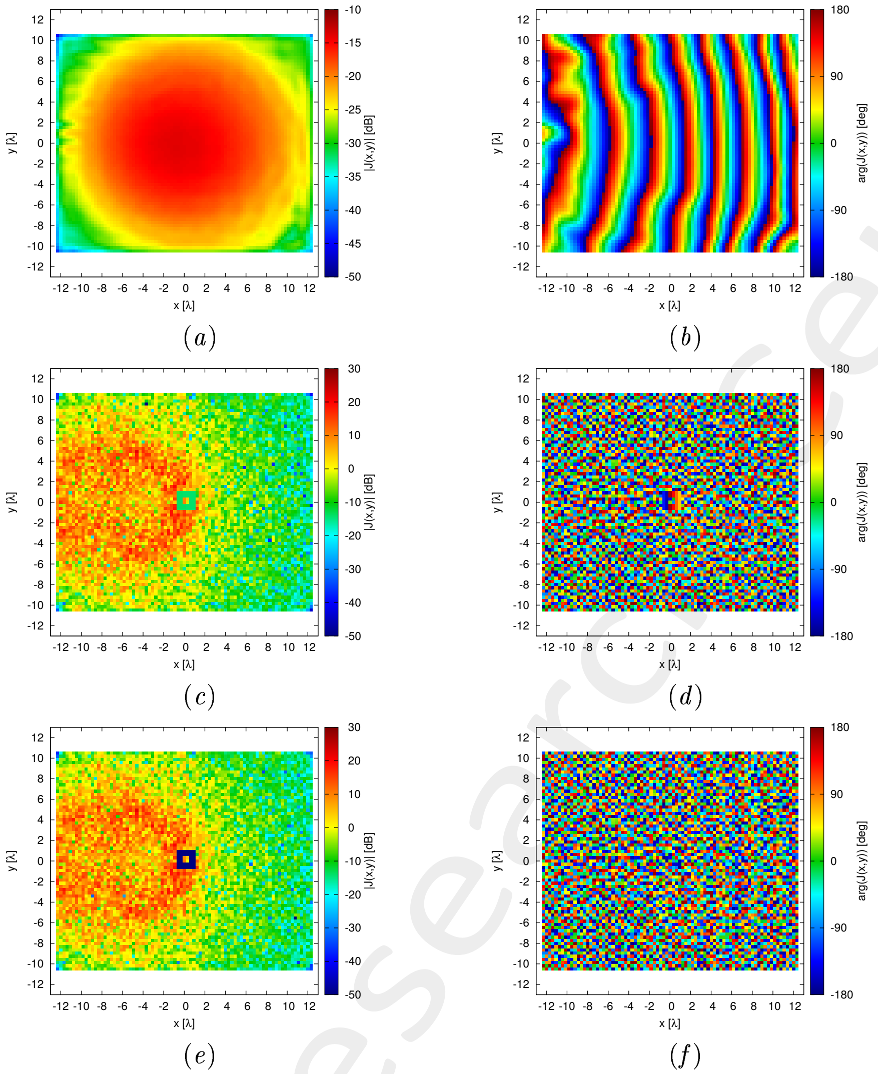

Figure 3: $(a)(c)(e)$ Magnitude and $(b)(d)(f)$ phase $(a)(b)$ of $J^{MN}(x,y)$, $(c)(d)$ $J^{NR}(x,y;\underline{\alpha})$, and $(e)(f)$ $J^{TOT}(x,y;\underline{\alpha})$.

Radiated Field

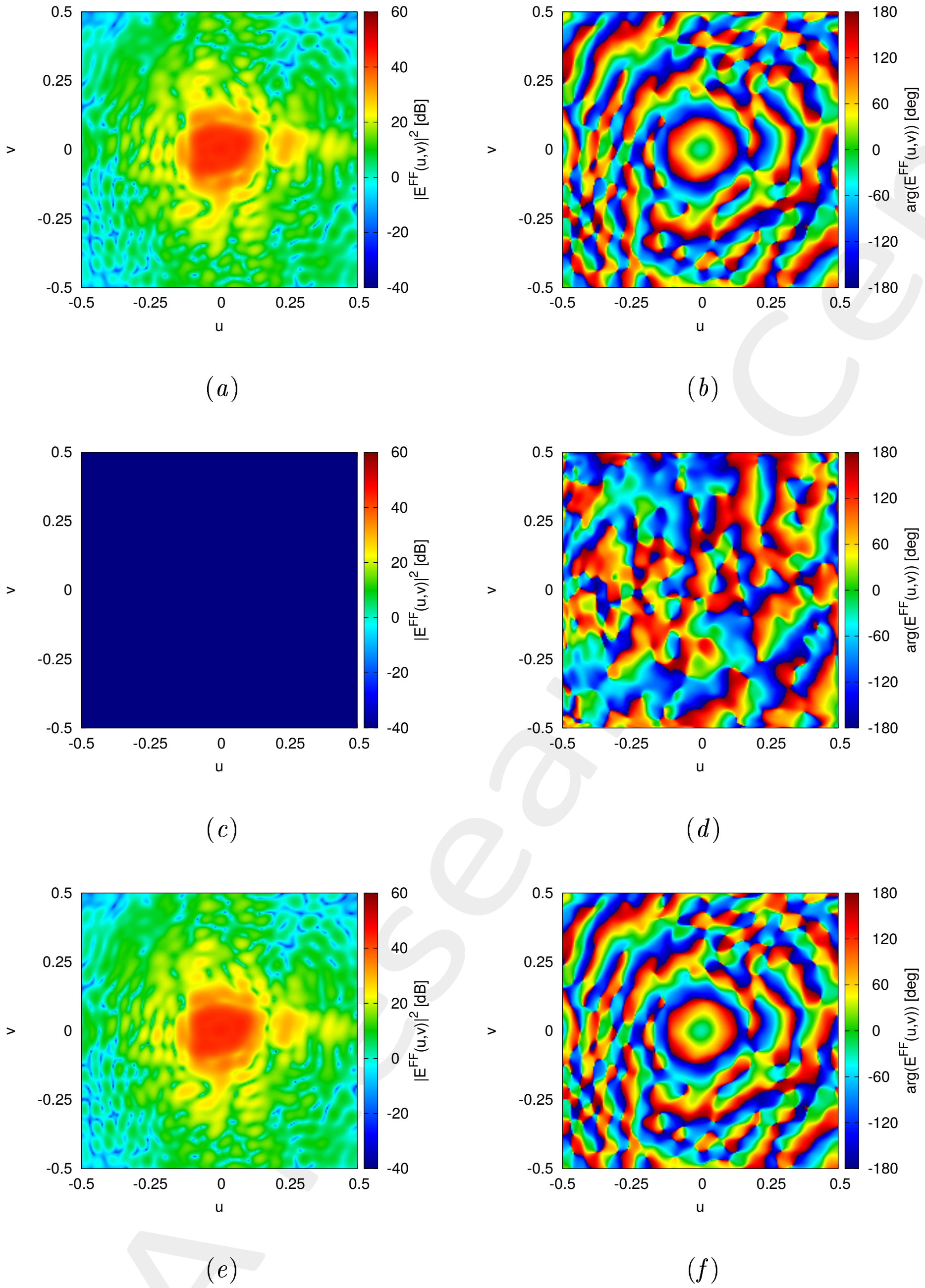

Figure 4: $(a)(c)(e)$ Magnitude and $(b)(d)(f)$ phase of the radiated field by $(a)(b)$, $J^{MN}(x,y)$, $(c)(d)$ $J^{NR}(x,y;\underline{\alpha})$, and $(e)(f)$ $J^{TOT}(x,y;\underline{\alpha})$.

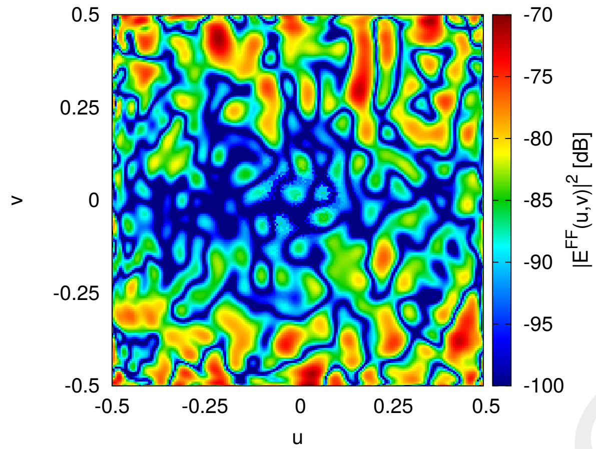

Figure 5: Magnitude of the difference between the radiated fields by $J^{MN}(x,y)$ and $J^{TOT}(x,y;\underline{\alpha})$.

1.2 Shape - "2 O LCD-Like @ Center and up right corner"

Parameters

- Number of reflectarray elements: $M = 81$, $N = 69$;
- Operative frequency: $f = 3.6$ [GHz];
- Polarization: L-CO;
- Number of elements in the forbidden region: $Q = 44$;

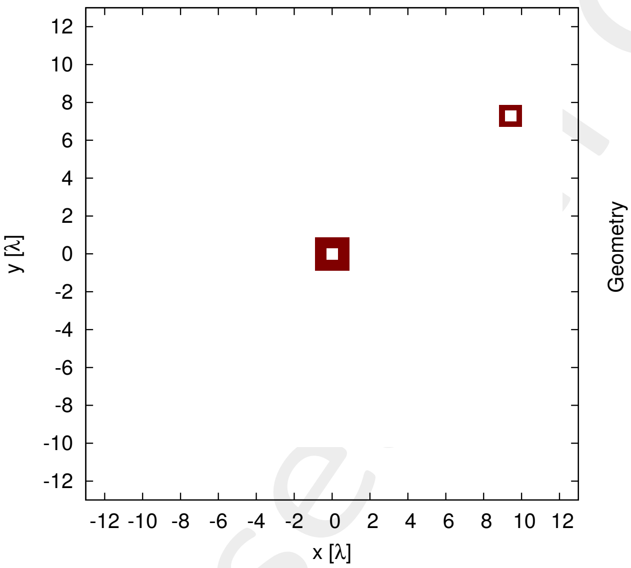

Figure 6: Geometry of forbidden region Ω.

Results

Magnitude and phase of the *NR* coefficients.

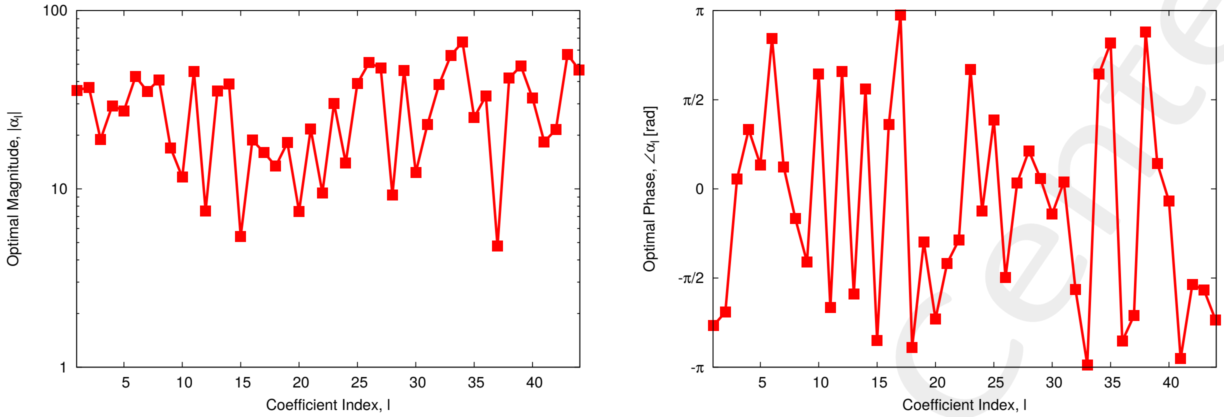

(a) (b)

Figure 7: Magnitude (a) and phase (b) of the solution.

Index q	$\Re\{\alpha_q\}$	$\Im\{\alpha_q\}$	Index q	$\Re\{\alpha_q\}$	$\Im\{\alpha_q\}$	Index q	$\Re\{\alpha_q\}$	$\Im\{\alpha_q\}$
1	-2.64×10^1	-2.40×10^1	16	7.97	1.70×10^1	31	2.28×10^1	2.78
2	-2.10×10^1	-3.06×10^1	17	-1.60×10^1	1.22	32	-7.82	-3.77×10^1
3	1.87×10^1	3.30	18	-1.26×10^1	-4.58	33	-5.60×10^1	-2.44
4	1.47×10^1	2.53×10^1	19	1.08×10^1	-1.47×10^1	34	-2.93×10^1	5.98×10^1
5	2.50×10^1	1.13×10^1	20	-4.94	-5.61	35	-2.11×10^1	1.36×10^1
6	-3.77×10^1	2.00×10^1	21	5.60	-2.09×10^1	36	-2.98×10^1	-1.47×10^1
7	3.26×10^1	1.34×10^1	22	5.90	-7.46	37	-2.93	-3.77
8	3.54×10^1	-2.05×10^1	23	-1.54×10^1	2.59×10^1	38	-3.89×10^1	1.52×10^1
9	4.70	-1.63×10^1	24	1.29×10^1	-5.31	39	4.41×10^1	2.12×10^1
10	-5.08	1.05×10^1	25	1.36×10^1	3.66×10^1	40	3.15×10^1	-6.91
11	-2.25×10^1	-3.97×10^1	26	4.36×10^{-1}	-5.11×10^1	41	-1.82×10^1	-2.73
12	-3.57	6.64	27	4.73×10^1	5.10	42	-2.48	-2.13×10^1
13	-9.85	-3.39×10^1	28	7.22	5.72	43	-1.19×10^1	-5.55×10^1
14	-7.22	3.80×10^1	29	4.55×10^1	8.27	44	-3.14×10^1	-3.43×10^1
15	-4.82	-2.48	30	1.12×10^1	-5.25			

Table II: Solution of the linear system

Currents Distribution

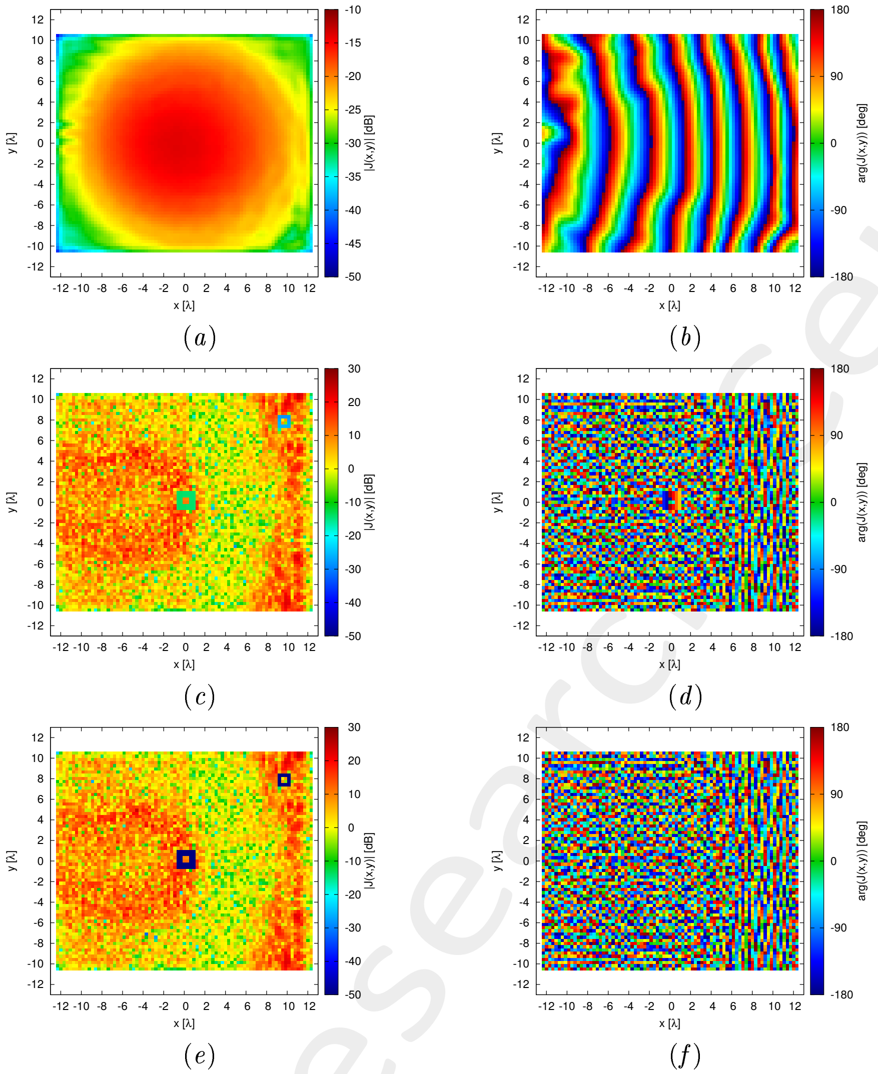

Figure 8: $(a)(c)(e)$ Magnitude and $(b)(d)(f)$ phase $(a)(b)$ of $J^{MN}(x,y)$, $(c)(d)$ $J^{NR}(x,y;\underline{\alpha})$, and $(e)(f)$ $J^{TOT}(x,y;\underline{\alpha})$.

Radiated Field

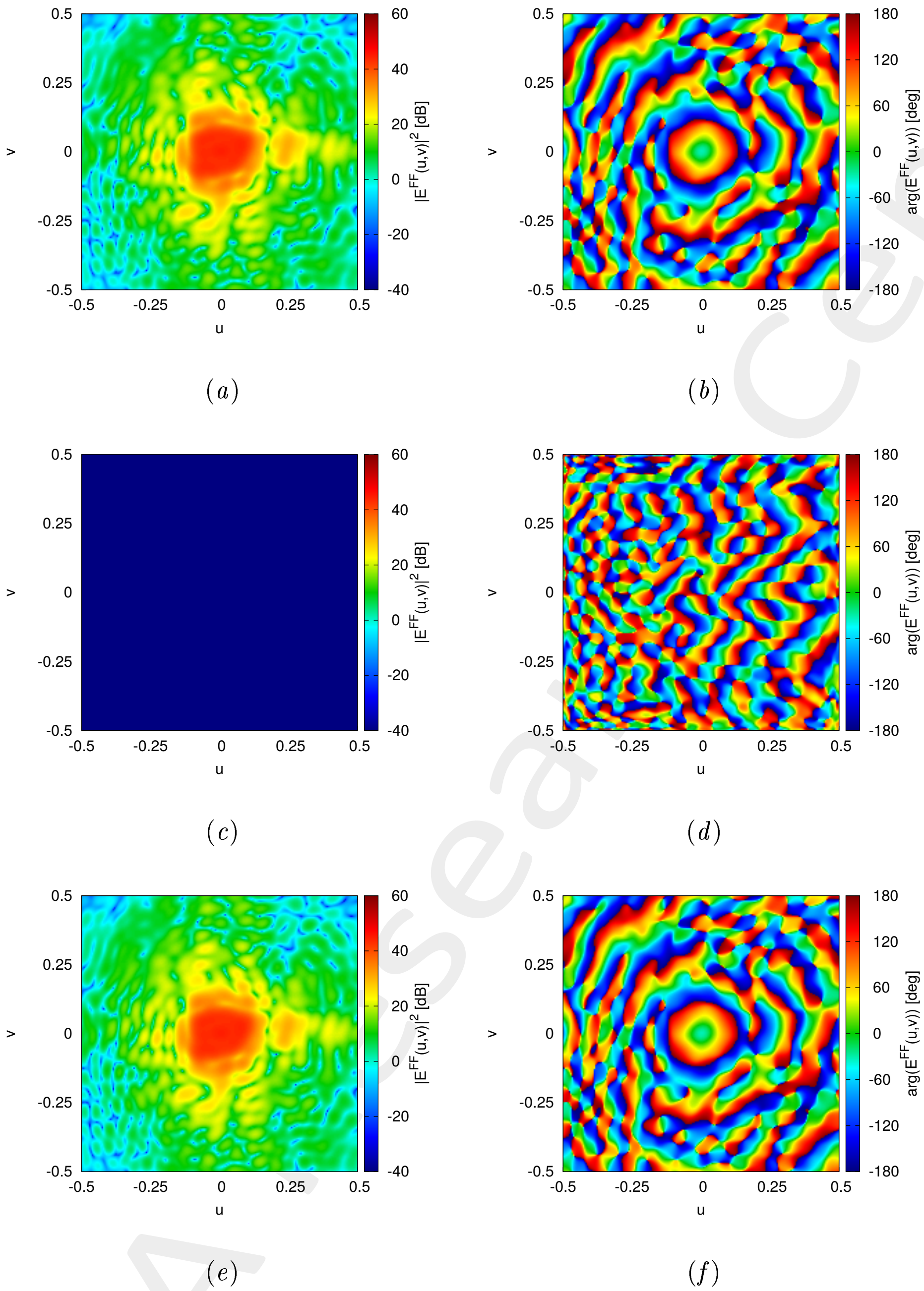

Figure 9: $(a)(c)(e)$ Magnitude and $(b)(d)(f)$ phase of the radiated field by $(a)(b)$, $J^{MN}(x, y)$, $(c)(d)$ $J^{NR}(x, y; \underline{\alpha})$, and $(e)(f)$ $J^{TOT}(x, y; \underline{\alpha})$.

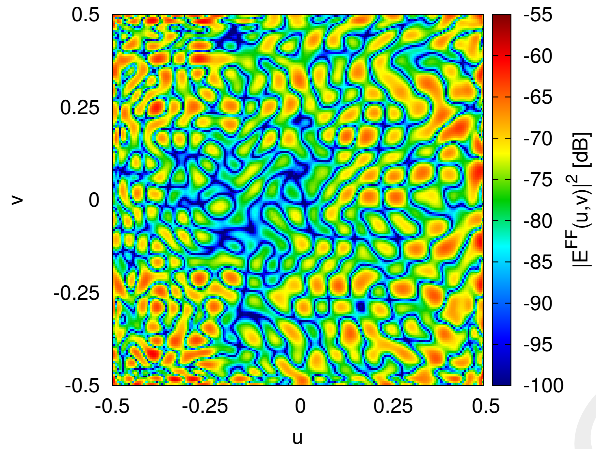

Figure 10: Magnitude of the difference between the radiated fields by $J^{MN}(x,y)$ and $J^{TOT}(x,y;\underline{\alpha})$.

1.3 Shape "O @ Center"

Parameters

- Number of reflectarray elements: $M = 81$, $N = 69$;
- Operative frequency: $f = 3.6$ [GHz];
- Polarization: L-CO;
- Number of elements in the forbidden region: $Q = 24$;

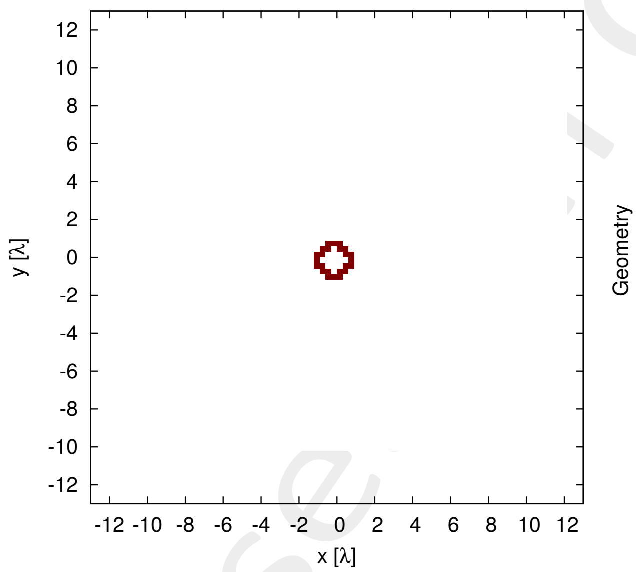

Figure 11: Geometry of forbidden region Ω.

Results

Magnitude and phase of the *NR* coefficients.

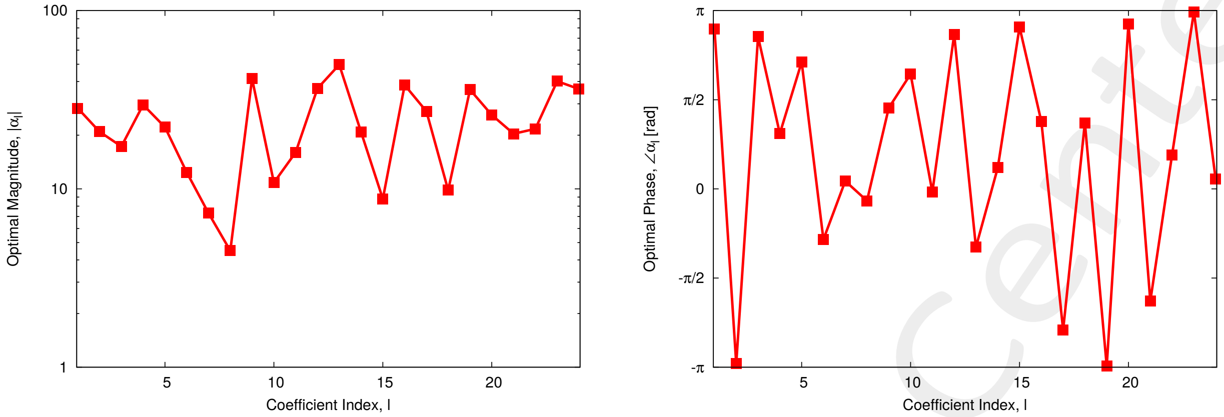

(a) (b)

Figure 12: Magnitude (a) and phase (b) of the solution.

Index q	$\Re\{\alpha_q\}$	$\Im\{\alpha_q\}$	Index q	$\Re\{\alpha_q\}$	$\Im\{\alpha_q\}$
1	-2.68×10^1	9.09	13	2.58×10^1	-4.25×10^1
2	-2.09×10^1	-1.29	14	1.94×10^1	7.59
3	-1.55×10^1	7.69	15	-8.42	2.52
4	1.66×10^1	2.45×10^1	16	1.44×10^1	3.54×10^1
5	-1.37×10^1	1.75×10^1	17	-2.16×10^1	-1.66×10^1
6	7.78	-9.64	18	3.90	9.02
7	7.24	1.01	19	-3.60×10^1	-7.66×10^{-1}
8	4.40	-9.34×10^{-1}	20	-2.53×10^1	5.98
9	5.94	4.11×10^1	21	-8.06	-1.87×10^1
10	-4.74	9.75	22	1.79×10^1	1.23×10^1
11	1.60×10^1	-8.90×10^{-1}	23	-4.02×10^1	8.72×10^{-1}
12	-3.34×10^1	1.50×10^1	24	3.58×10^1	6.35

Table III: Solution of the linear system.

Currents Distribution

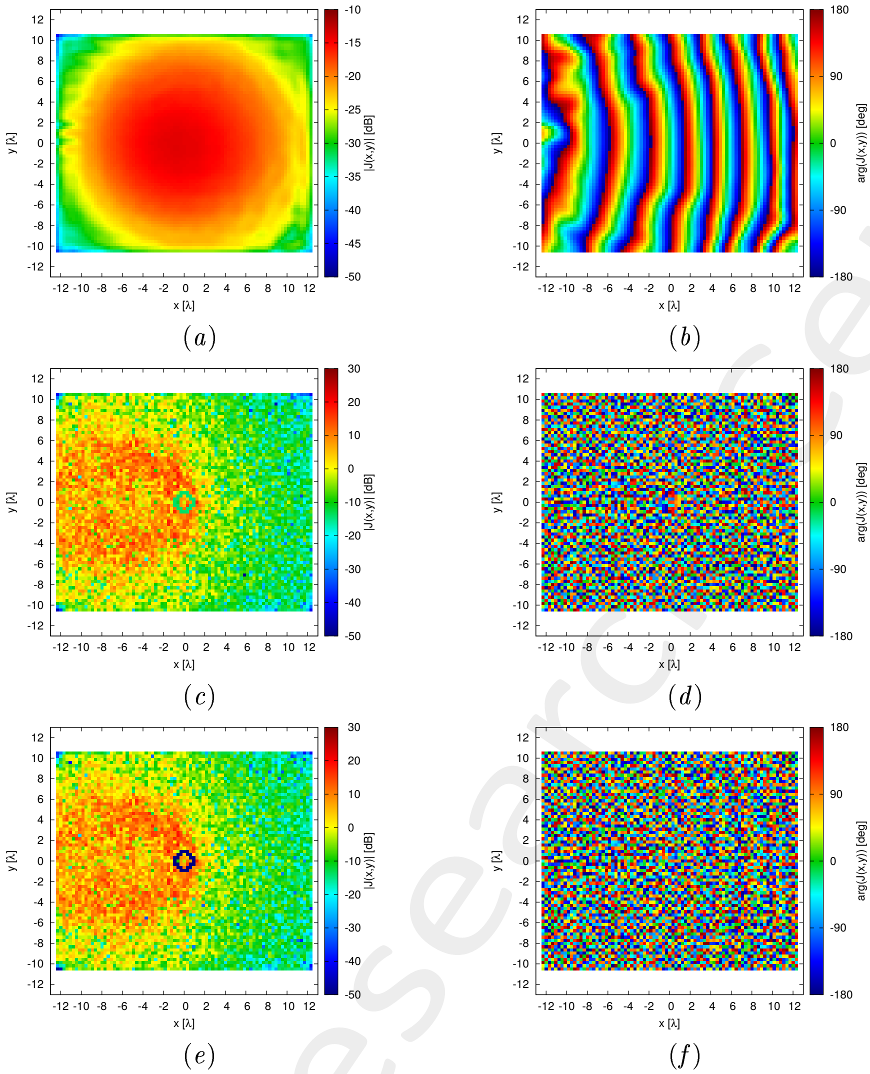

Figure 13: $(a)(c)(e)$ Magnitude and $(b)(d)(f)$ phase $(a)(b)$ of $J^{MN}(x,y)$, $(c)(d)$ $J^{NR}(x,y;\underline{\alpha})$, and $(e)(f)$ $J^{TOT}(x,y;\underline{\alpha})$.

Radiated Field

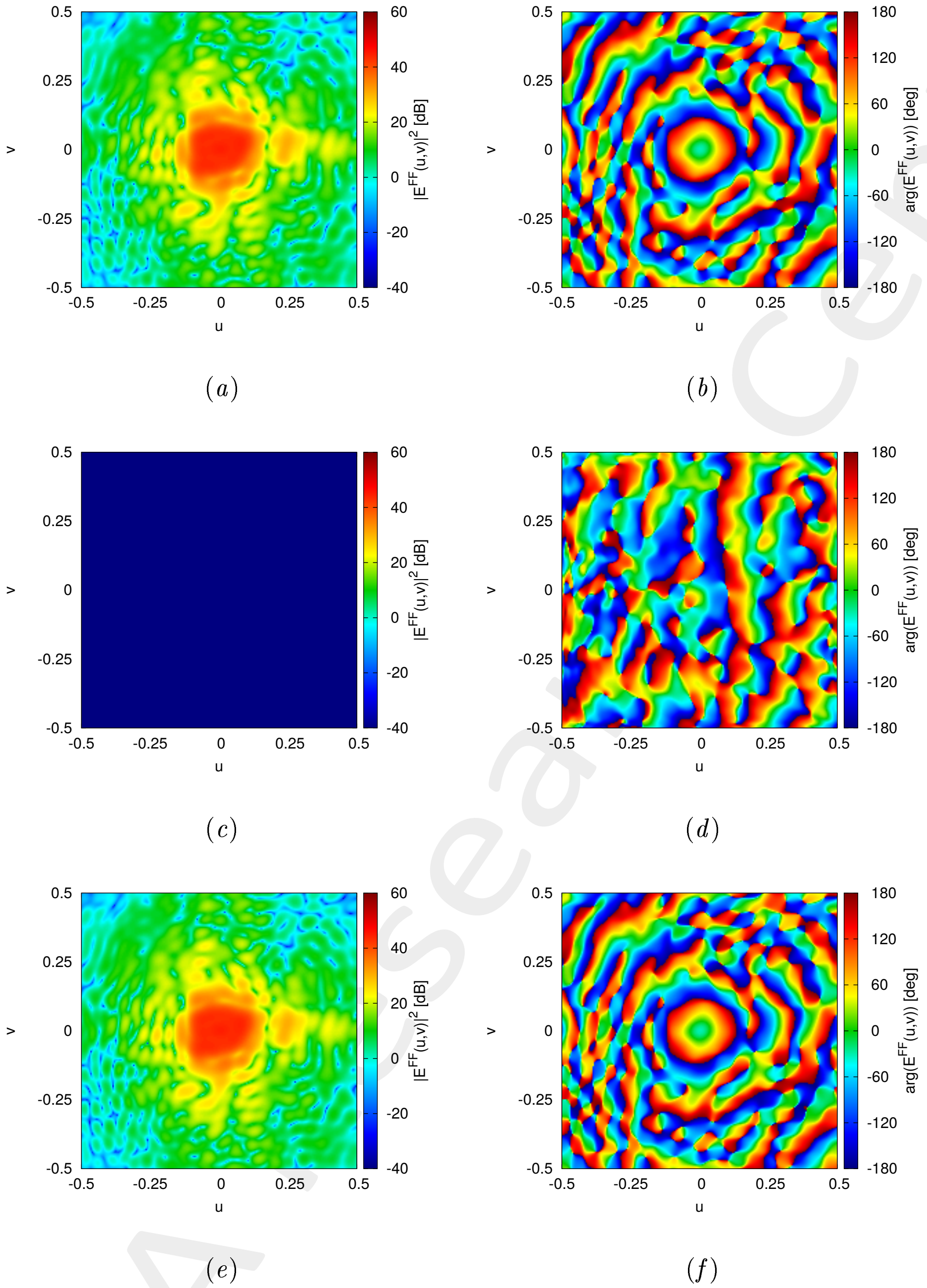

Figure 14: $(a)(c)(e)$ Magnitude and $(b)(d)(f)$ phase of the radiated field by $(a)(b)$, $J^{MN}(x, y)$, $(c)(d)$ $J^{NR}(x, y; \underline{\alpha})$, and $(e)(f)$ $J^{TOT}(x, y; \underline{\alpha})$.

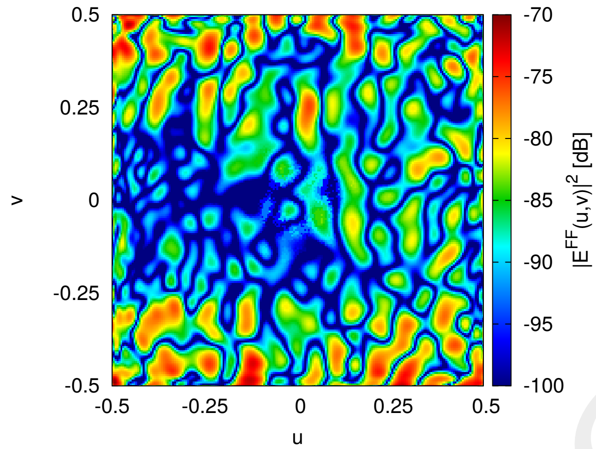

Figure 15: Magnitude of the difference between the radiated fields by $J^{MN}(x,y)$ and $J^{TOT}(x,y;\underline{\alpha})$.

1.4 Shape "2 O @ Center and up right corner"

Parameters

- Number of reflectarray elements: $M = 81$, $N = 69$;
- Operative frequency: $f = 3.6$ [GHz];
- Polarization: L-CO;
- Number of elements in the forbidden region: $Q = 36$;

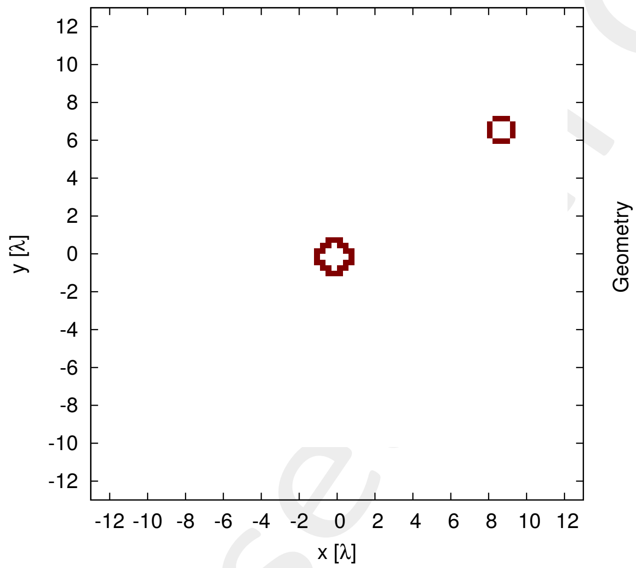

Figure 16: Geometry of forbidden region Ω.

Results

Magnitude and phase of the *NR* coefficients.

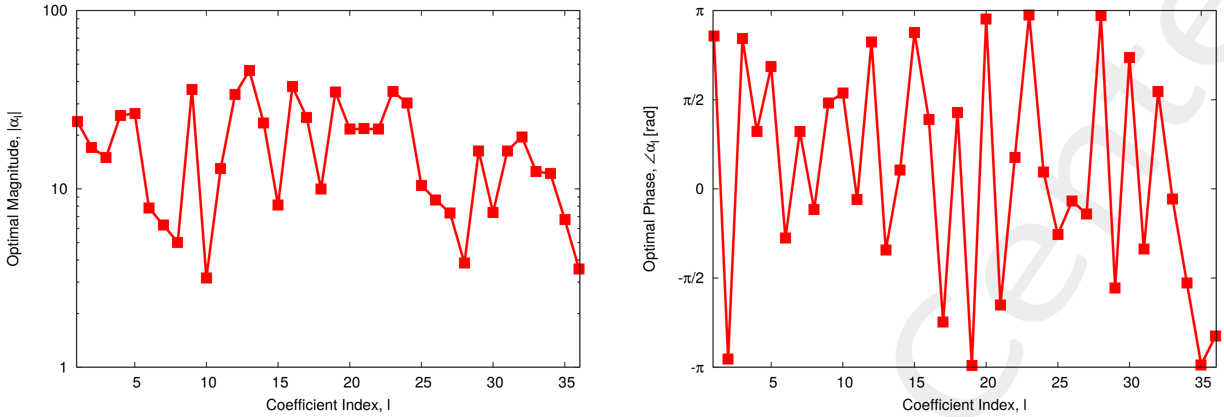

(a) (b)

Figure 17: Magnitude (a) and phase (b) of the solution.

Index q	$\Re\{\alpha_q\}$	$\Im\{\alpha_q\}$	Index q	$\Re\{\alpha_q\}$	$\Im\{\alpha_q\}$	Index q	$\Re\{\alpha_q\}$	$\Im\{\alpha_q\}$
1	-2.15×10^{1}	1.03×10^{1}	13	2.18×10^{1}	-4.06×10^{1}	25	7.24	-7.55
2	-1.69×10^{1}	-2.51	14	2.22×10^{1}	7.71	26	8.48	-1.81
3	-1.32×10^{1}	7.15	15	-7.50	3.05	27	6.63	-3.14
4	1.36×10^{1}	2.20×10^{1}	16	1.27×10^{1}	3.52×10^{1}	28	-3.82	3.26×10^{-1}
5	-1.46×10^{1}	2.21×10^{1}	17	-1.77×10^{1}	-1.80×10^{1}	29	-2.90	-1.61×10^{1}
6	5.06	-5.96	18	2.23	9.73	30	-5.00	5.43
7	3.35	5.30	19	-3.49×10^{1}	-1.15	31	7.96	-1.43×10^{1}
8	4.69	-1.78	20	-2.14×10^{1}	3.23	32	-2.77	1.94×10^{1}
9	1.93	3.61×10^{1}	21	-9.93	-1.94×10^{1}	33	1.24×10^{1}	-2.18
10	-3.83×10^{-1}	3.15	22	1.84×10^{1}	1.14×10^{1}	34	-1.01	-1.21×10^{1}
11	1.28×10^{1}	-2.45	23	-3.50×10^{1}	2.67	35	-6.75	-2.93×10^{-1}
12	-2.88×10^{1}	1.77×10^{1}	24	2.90×10^{1}	8.91	36	-3.03	-1.86

Table IV: Solution of the linear system.

Currents Distribution

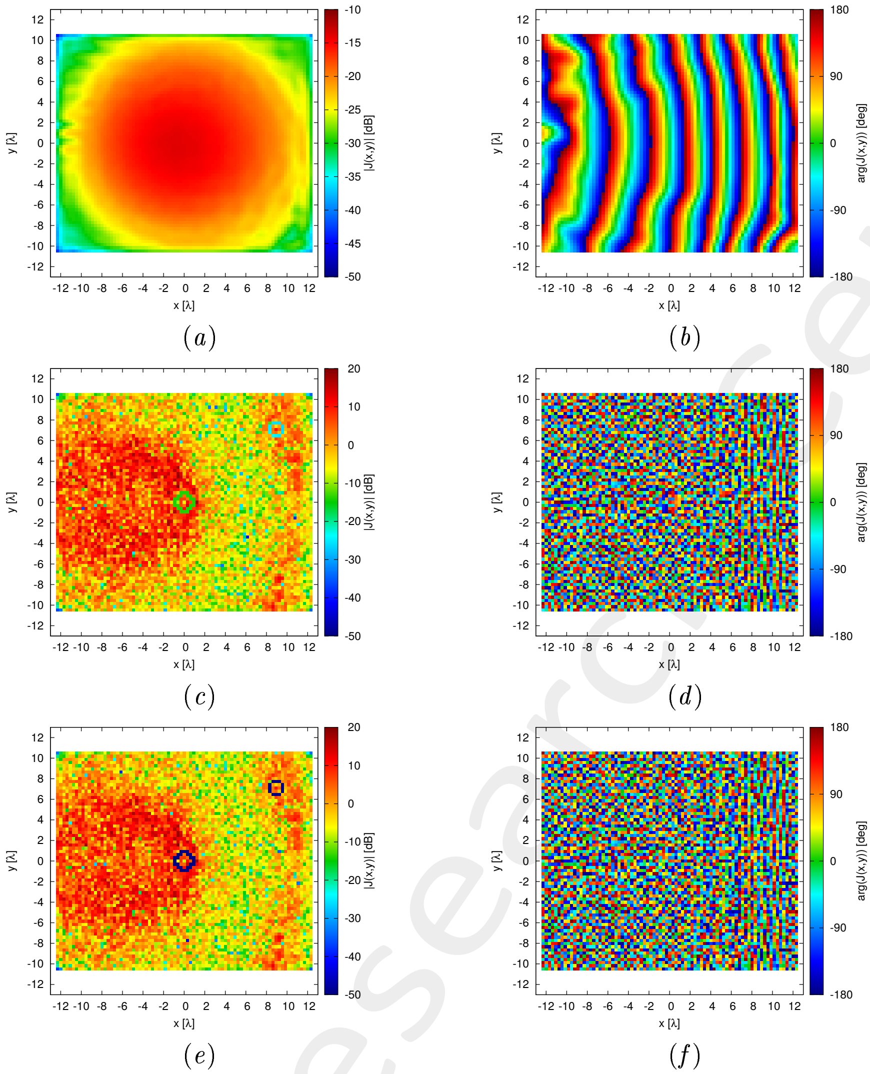

Figure 18: $(a)(c)(e)$ Magnitude and $(b)(d)(f)$ phase $(a)(b)$ of $J^{MN}(x,y)$, $(c)(d)$ $J^{NR}(x,y;\underline{\alpha})$, and $(e)(f)$ $J^{TOT}(x,y;\underline{\alpha})$.

Radiated Field

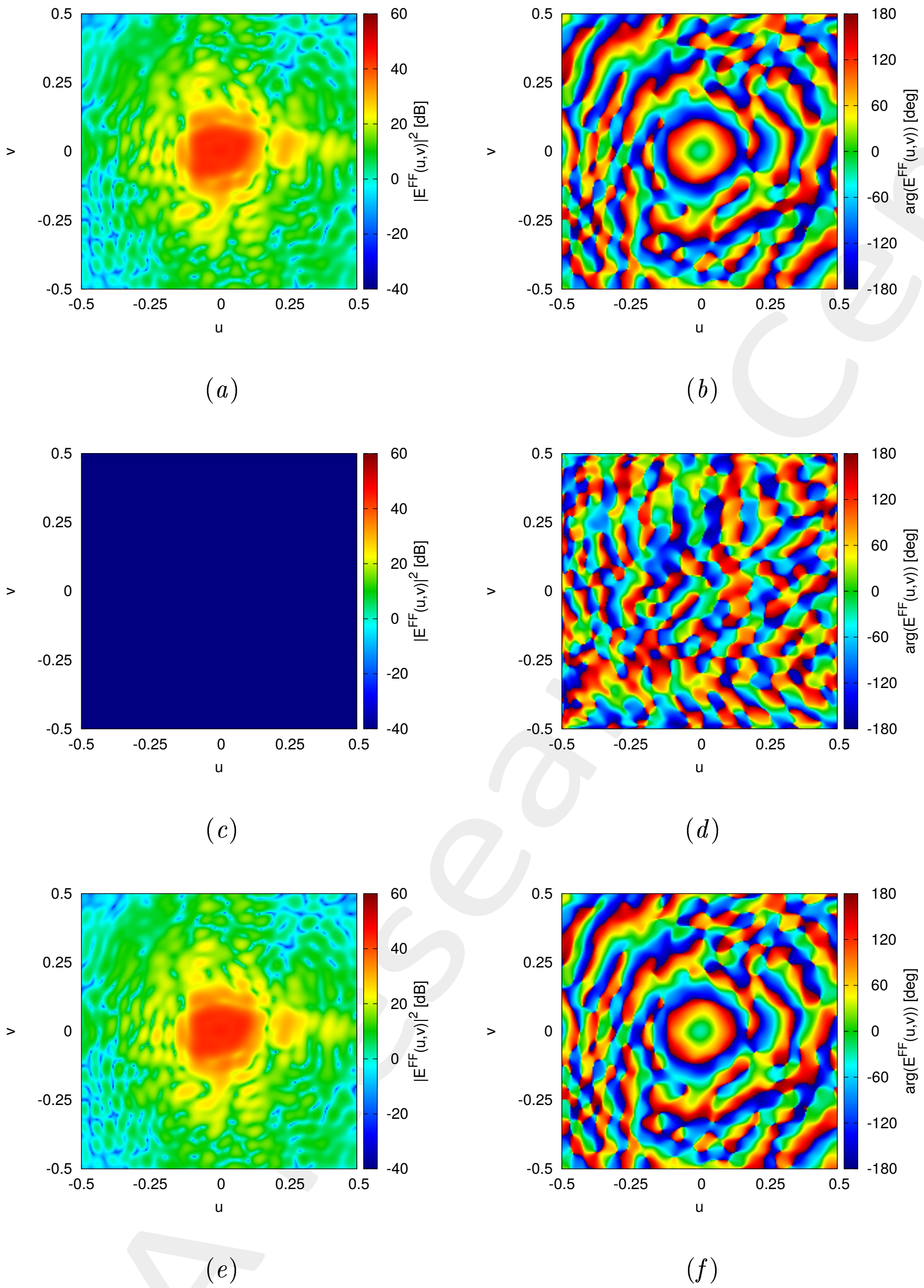

Figure 19: $(a)(c)(e)$ Magnitude and $(b)(d)(f)$ phase of the radiated field by $(a)(b)$, $J^{MN}(x,y)$, $(c)(d)$ $J^{NR}(x,y;\underline{\alpha})$, and $(e)(f)$ $J^{TOT}(x,y;\underline{\alpha})$.

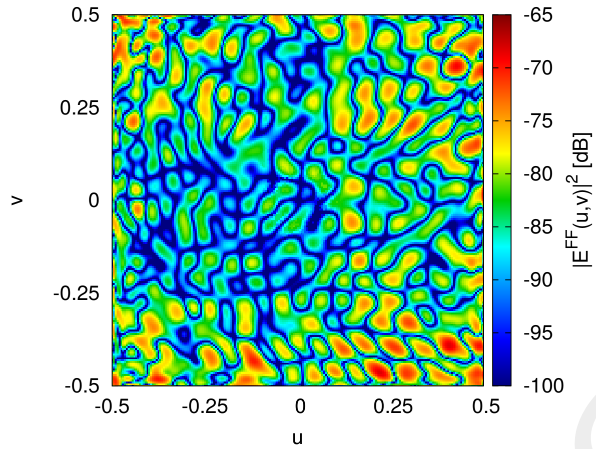

Figure 20: Magnitude of the difference between the radiated fields by $J^{MN}(x,y)$ and $J^{TOT}(x,y;\underline{\alpha})$.

1.5 Shape "Circle @ Center"

Parameters

- Number of reflectarray elements: $M = 81$, $N = 69$;
- Operative frequency: $f = 3.6$ [GHz];
- Polarization: L-CO;
- Number of elements in the forbidden region: $Q = 37$;

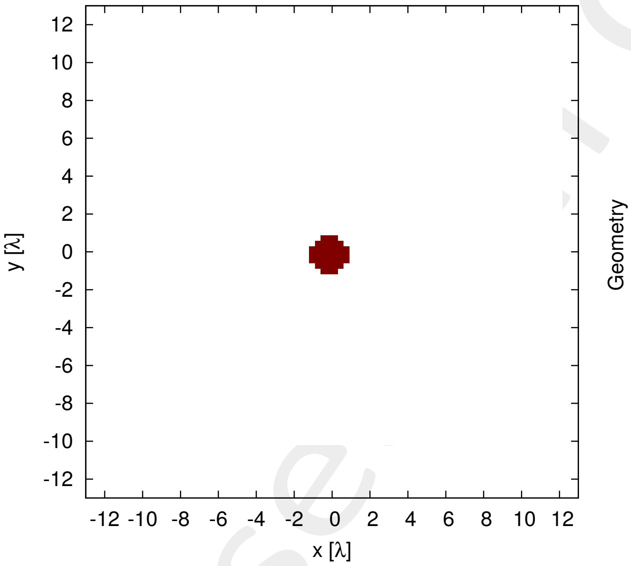

Figure 21: Geometry of forbidden region Ω.

Results

Magnitude and phase of the *NR* coefficients.

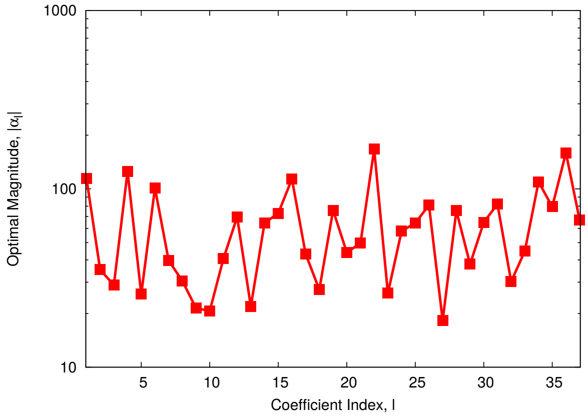

(a)

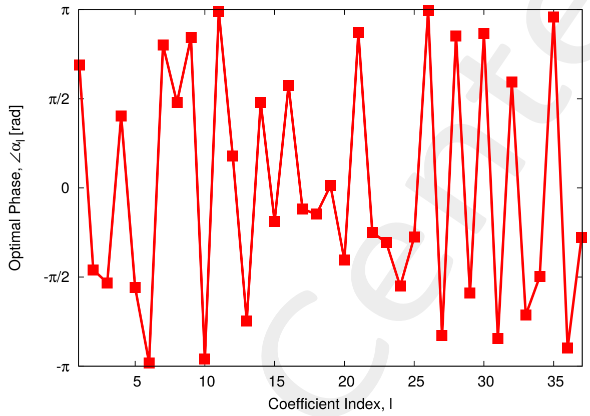

(b)

Figure 22: Magnitude (a) and phase (b) of the solution.

Index q	$\Re\{\alpha_q\}$	$\Im\{\alpha_q\}$	Index q	$\Re\{\alpha_q\}$	$\Im\{\alpha_q\}$	Index q	$\Re\{\alpha_q\}$	$\Im\{\alpha_q\}$
1	-6.39×10^1	9.49×10^1	14	4.04	6.42×10^1	26	-8.11×10^1	1.05
2	4.48	-3.49×10^1	15	6.06×10^1	-4.07×10^1	27	-1.57×10^1	-9.43
3	-2.94	-2.87×10^1	16	-2.67×10^1	1.10×10^2	28	-6.76×10^1	3.36×10^1
4	3.73×10^1	1.20×10^2	17	4.02×10^1	-1.57×10^1	29	-1.06×10^1	-3.63×10^1
5	-4.60	-2.53×10^1	18	2.44×10^1	-1.22×10^1	30	-5.91×10^1	2.67×10^1
6	-1.01×10^2	-6.07	19	7.58×10^1	3.10	31	-7.24×10^1	-3.89×10^1
7	-3.21×10^1	2.33×10^1	20	1.29×10^1	-4.21×10^1	32	-8.77	2.89×10^1
8	2.04	3.04×10^1	21	-4.56×10^1	1.96×10^1	33	-2.78×10^1	-3.51×10^1
9	-1.89×10^1	1.02×10^1	22	1.18×10^2	-1.18×10^2	34	6.91×10^{-1}	-1.10×10^2
10	-2.05×10^1	-2.58	23	1.48×10^1	-2.13×10^1	35	-7.88×10^1	1.01×10^1
11	-4.06×10^1	1.52	24	-9.27	-5.72×10^1	36	-1.52×10^2	-4.98×10^1
12	5.89×10^1	3.70×10^1	25	4.16×10^1	-4.92×10^1	37	4.31×10^1	-5.11×10^1
13	-1.53×10^1	-1.57×10^1						

Table V: Solution of the linear system.

Currents Distribution

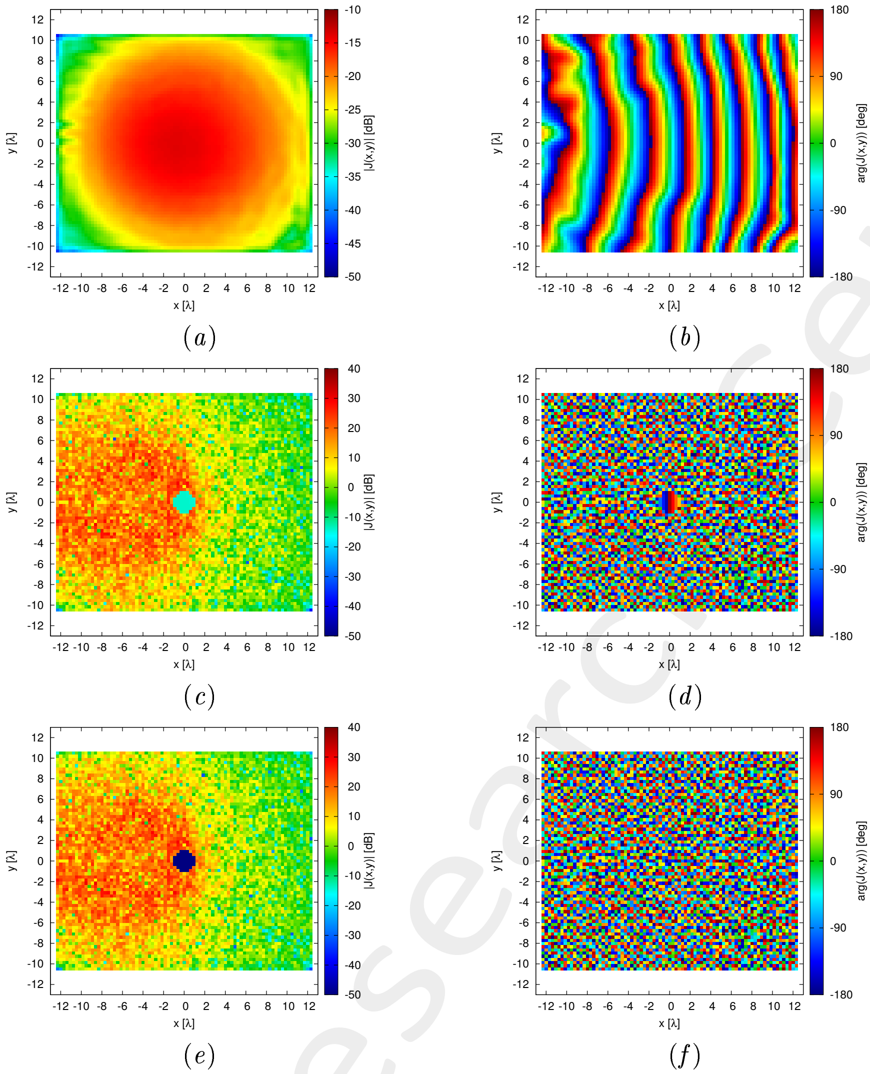

Figure 23: $(a)(c)(e)$ Magnitude and $(b)(d)(f)$ phase $(a)(b)$ of $J^{MN}(x,y)$, $(c)(d)$ $J^{NR}(x,y;\underline{\alpha})$, and $(e)(f)$ $J^{TOT}(x,y;\underline{\alpha})$.

Radiated Field

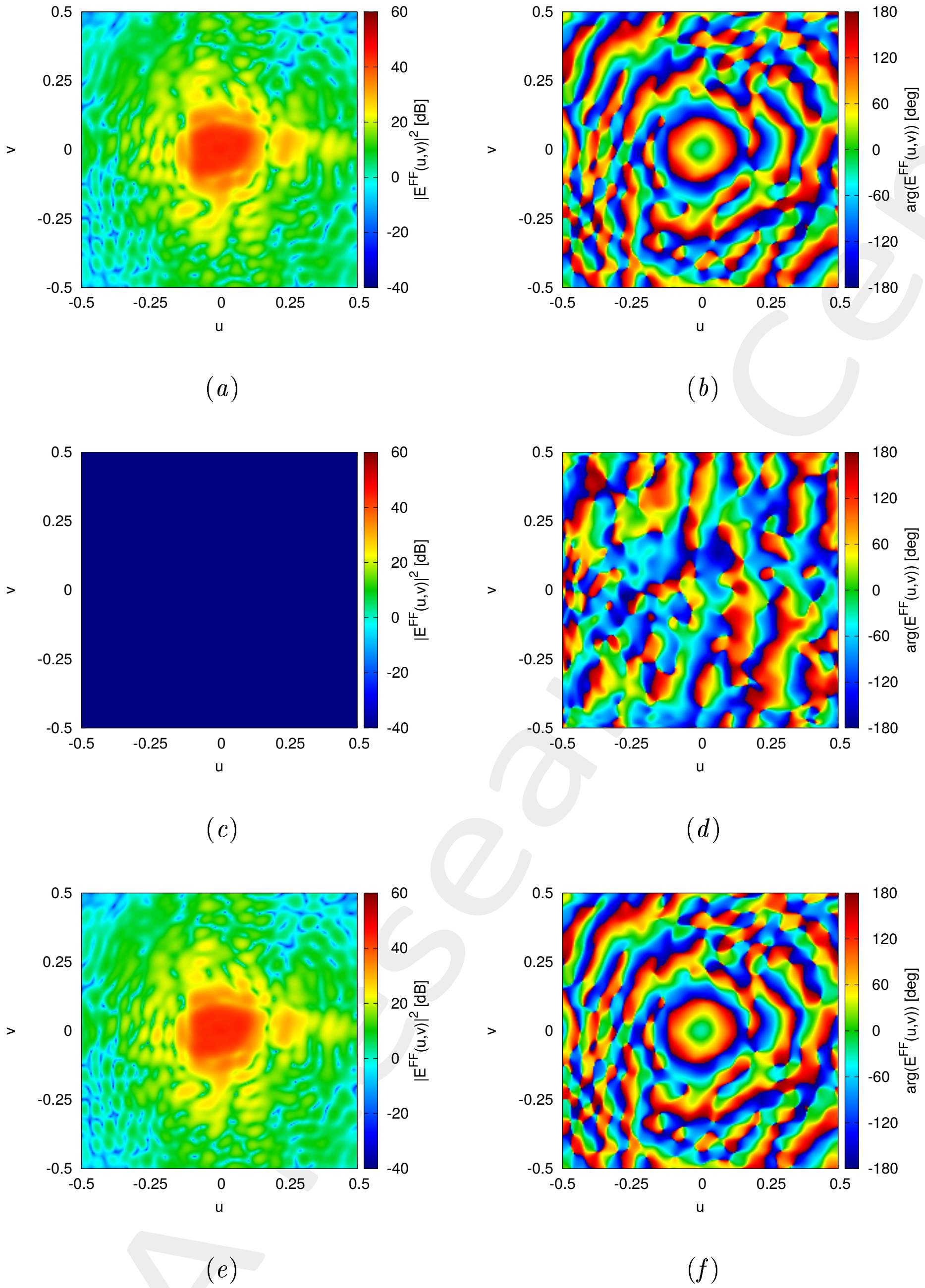

Figure 24: $(a)(c)(e)$ Magnitude and $(b)(d)(f)$ phase of the radiated field by $(a)(b)$, $J^{MN}(x,y)$, $(c)(d)$ $J^{NR}(x,y;\underline{\alpha})$, and $(e)(f)$ $J^{TOT}(x,y;\underline{\alpha})$.

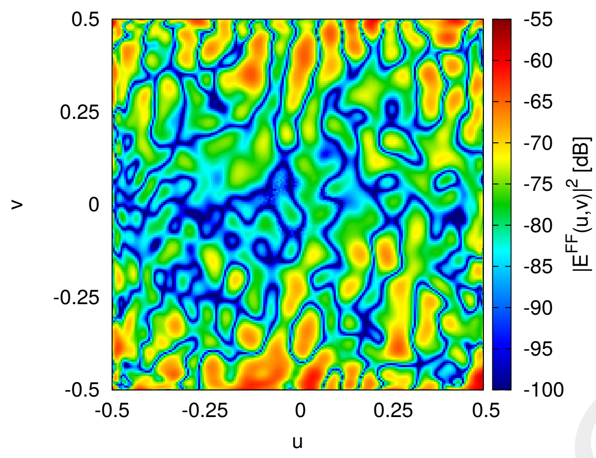

Figure 25: Magnitude of the difference between the radiated fields by $J^{MN}(x,y)$ and $J^{TOT}(x,y;\underline{\alpha})$.

1.6 Shape "2 Circle @ Center and up right corner"

Parameters

- Number of reflectarray elements: $M = 81$, $N = 69$;
- Operative frequency: $f = 3.6$ [GHz];
- Polarization: L-CO;
- Number of elements in the forbidden region: $Q = 58$;

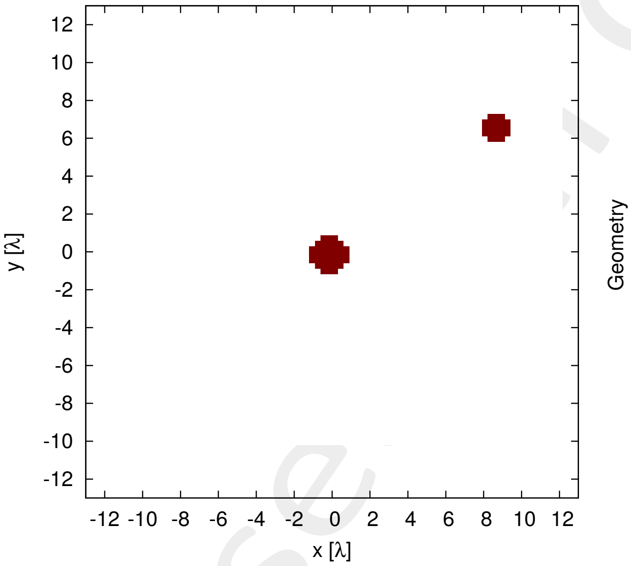

Figure 26: Geometry of forbidden region Ω.

Results

Magnitude and phase of the *NR* coefficients.

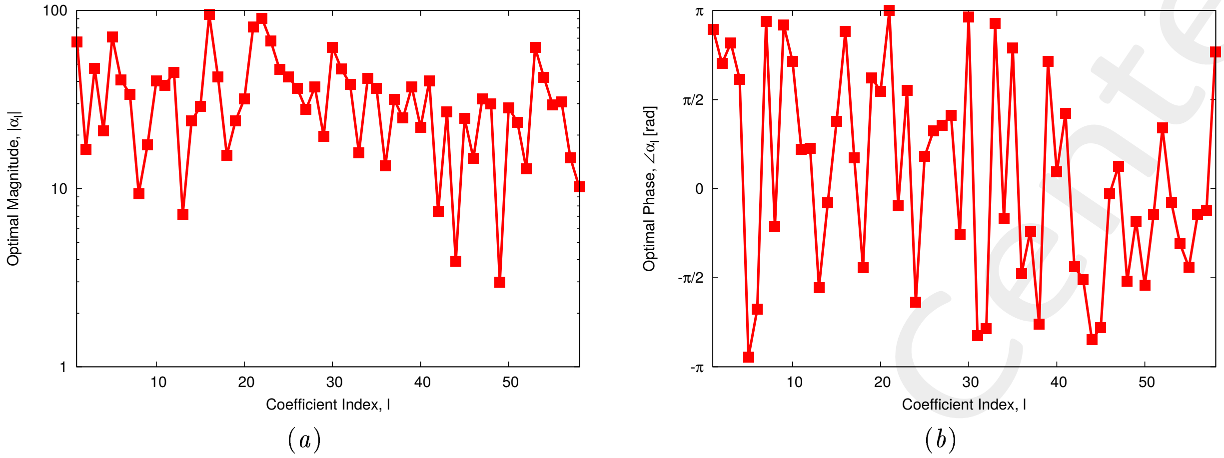

Figure 27: Magnitude (a) and phase (b) of the solution.

Index q	$\Re\{\alpha_q\}$	$\Im\{\alpha_q\}$	Index q	$\Re\{\alpha_q\}$	$\Im\{\alpha_q\}$	Index q	$\Re\{\alpha_q\}$	$\Im\{\alpha_q\}$
1	-6.30×10^{1}	2.22×10^{1}	21	-8.09×10^{1}	1.72×10^{-1}	40	2.12×10^{1}	6.45
2	-9.91	1.34×10^{1}	22	8.64×10^{1}	-2.69×10^{1}	41	9.53	3.92×10^{1}
3	-3.99×10^{1}	2.56×10^{1}	23	-1.08×10^{1}	6.64×10^{1}	42	1.46	-7.26
4	-7.47	1.98×10^{1}	24	-1.96×10^{1}	-4.24×10^{1}	43	-8.66×10^{-1}	-2.69×10^{1}
5	-7.01×10^{1}	-1.22×10^{1}	25	3.57×10^{1}	2.28×10^{1}	44	-3.47	-1.80
6	-2.15×10^{1}	-3.47×10^{1}	26	1.92×10^{1}	3.11×10^{1}	45	-1.91×10^{1}	-1.59×10^{1}
7	-3.33×10^{1}	6.38	27	1.22×10^{1}	2.51×10^{1}	46	1.47×10^{1}	-1.32
8	7.39	-5.79	28	1.01×10^{1}	3.58×10^{1}	47	2.95×10^{1}	1.22×10^{1}
9	-1.71×10^{1}	4.45	29	1.37×10^{1}	-1.41×10^{1}	48	-1.94	-2.98×10^{1}
10	-2.52×10^{1}	3.14×10^{1}	30	-6.18×10^{1}	6.89	49	2.52	-1.62
11	2.94×10^{1}	2.43×10^{1}	31	-4.02×10^{1}	-2.46×10^{1}	50	-3.74	-2.82×10^{1}
12	3.42×10^{1}	2.93×10^{1}	32	-3.01×10^{1}	-2.42×10^{1}	51	2.13×10^{1}	-1.03×10^{1}
13	-1.22	-7.10	33	-1.55×10^{1}	3.56	52	6.19	1.14×10^{1}
14	2.33×10^{1}	-5.96	34	3.58×10^{1}	-2.11×10^{1}	53	6.03×10^{1}	-1.46×10^{1}
15	1.08×10^{1}	2.68×10^{1}	35	-2.90×10^{1}	2.23×10^{1}	54	2.37×10^{1}	-3.49×10^{1}
16	-8.86×10^{1}	3.38×10^{1}	36	1.01	-1.34×10^{1}	55	5.36	-2.90×10^{1}
17	3.61×10^{1}	2.20×10^{1}	37	2.32×10^{1}	-2.16×10^{1}	56	2.77×10^{1}	-1.35×10^{1}
18	2.70	-1.52×10^{1}	38	-1.83×10^{1}	-1.70×10^{1}	57	1.39×10^{1}	-5.57
19	-9.09	2.23×10^{1}	39	-2.32×10^{1}	2.91×10^{1}	58	-7.62	6.86
20	-4.70	3.15×10^{1}						

Table VI: Solution of the linear system.

Currents Distribution

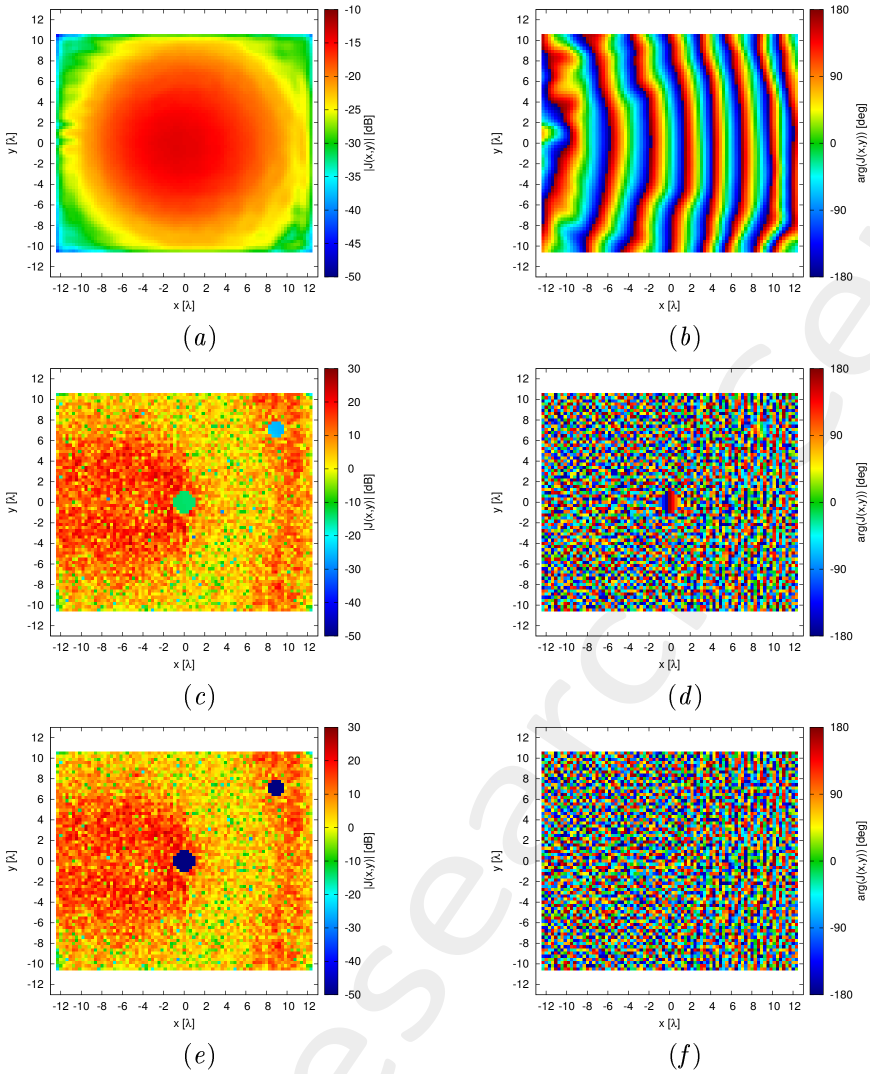

Figure 28: $(a)(c)(e)$ Magnitude and $(b)(d)(f)$ phase $(a)(b)$ of $J^{MN}(x,y)$, $(c)(d)$ $J^{NR}(x,y;\underline{\alpha})$, and $(e)(f)$ $J^{TOT}(x,y;\underline{\alpha})$.

Radiated Field

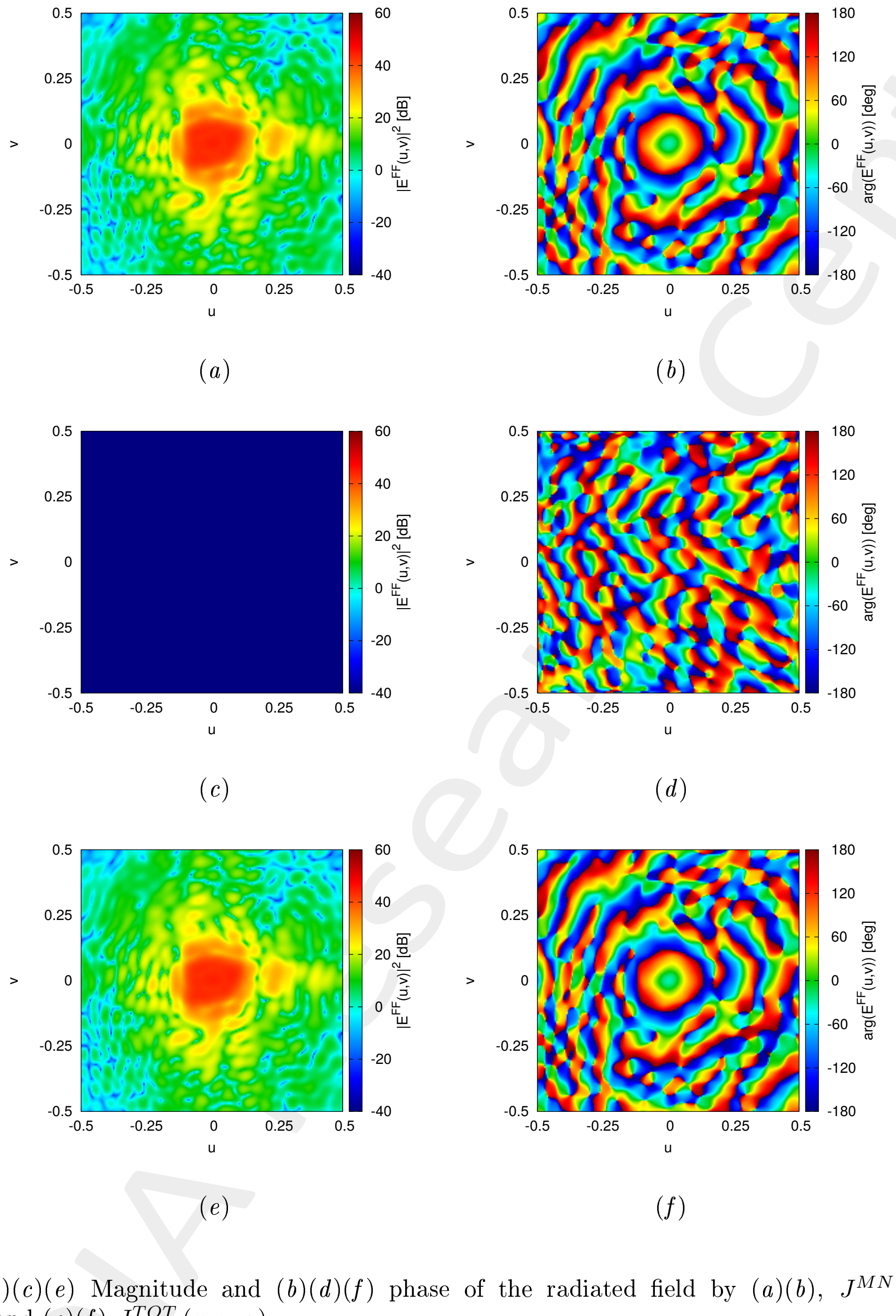

Figure 29: $(a)(c)(e)$ Magnitude and $(b)(d)(f)$ phase of the radiated field by $(a)(b)$, $J^{MN}(x,y)$, $(c)(d)$ $J^{NR}(x,y;\underline{\alpha})$, and $(e)(f)$ $J^{TOT}(x,y;\underline{\alpha})$.

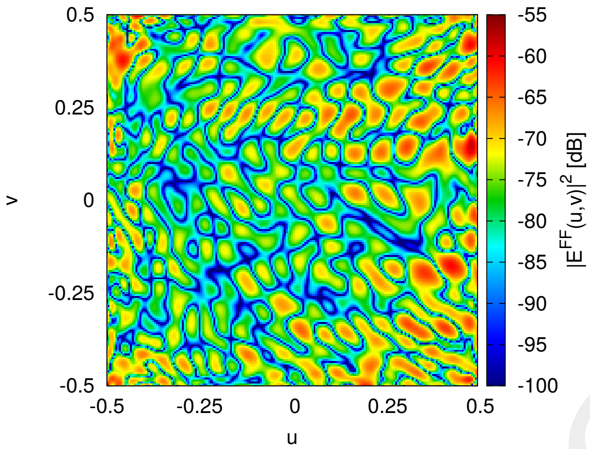

Figure 30: Magnitude of the difference between the radiated fields by $J^{MN}(x,y)$ and $J^{TOT}(x,y;\underline{\alpha})$.

1.7 Shape "Plus @ down left corner"

Parameters

- Number of reflectarray elements: $M = 81$, $N = 69$;
- Operative frequency: $f = 3.6$ [GHz];
- Polarization: L-CO;
- Number of elements in the forbidden region: $Q = 28$;

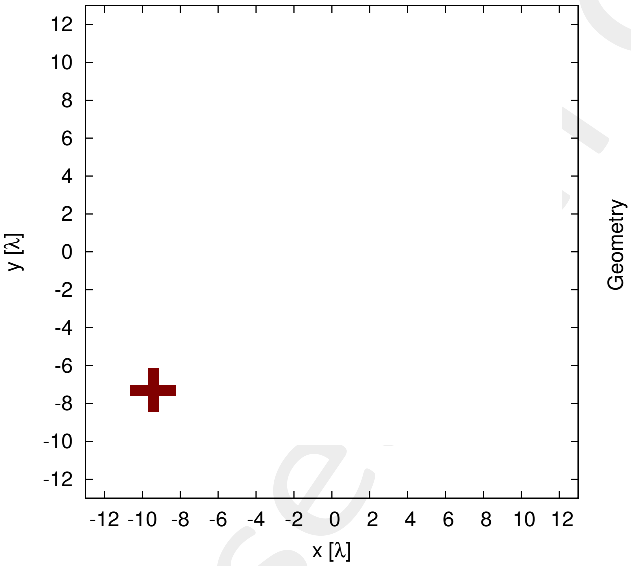

Figure 31: Geometry of forbidden region Ω.

Results

Magnitude and phase of the *NR* coefficients.

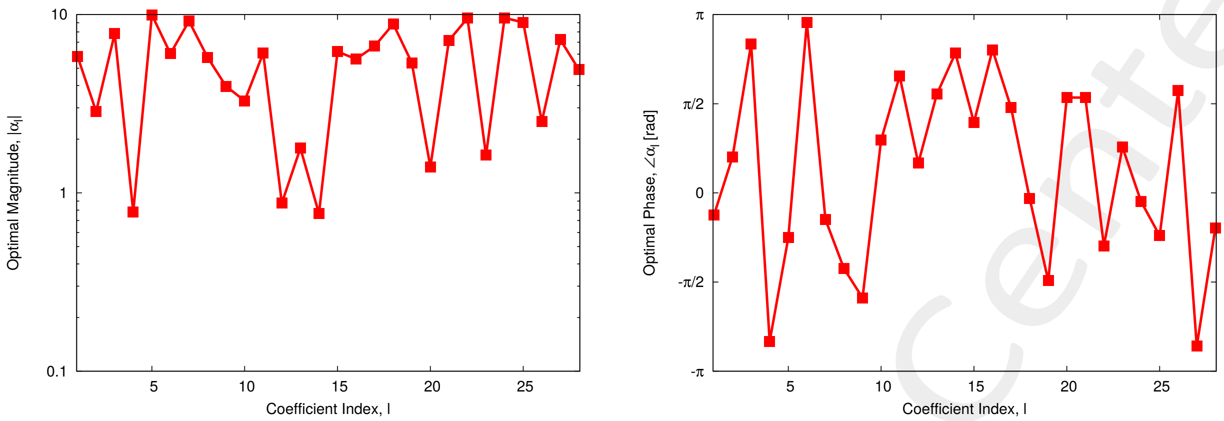

(a) (b)

Figure 32: Magnitude (a) and phase (b) of the solution.

Index q	$\Re\{\alpha_q\}$	$\Im\{\alpha_q\}$	Index q	$\Re\{\alpha_q\}$	$\Im\{\alpha_q\}$	Index q	$\Re\{\alpha_q\}$	$\Im\{\alpha_q\}$
1	5.39	-2.20	11	-2.84	5.38	20	-1.54×10^{-1}	1.39
2	2.30	1.70	12	7.60×10^{-1}	4.38×10^{-1}	21	-7.65×10^{-1}	7.12
3	-6.79	3.87	13	-2.98×10^{-1}	1.76	22	5.69	-7.66
4	-6.78×10^{-1}	-3.93×10^{-1}	14	-5.95×10^{-1}	4.82×10^{-1}	23	1.13	1.18
5	7.03	-7.07	15	2.00	5.87	24	9.47	-1.43
6	-5.98	8.36×10^{-1}	16	-4.59	3.27	25	6.60	-6.19
7	8.21	-4.14	17	4.62×10^{-1}	6.64	26	-5.79×10^{-1}	2.44
8	1.35	-5.59	18	8.81	-8.83×10^{-1}	27	-6.54	-3.11
9	-1.08	-3.81	19	1.37×10^{-1}	-5.36	28	3.99	-2.86
10	1.96	2.63						

Table VII: Solution of the linear system.

Currents Distribution

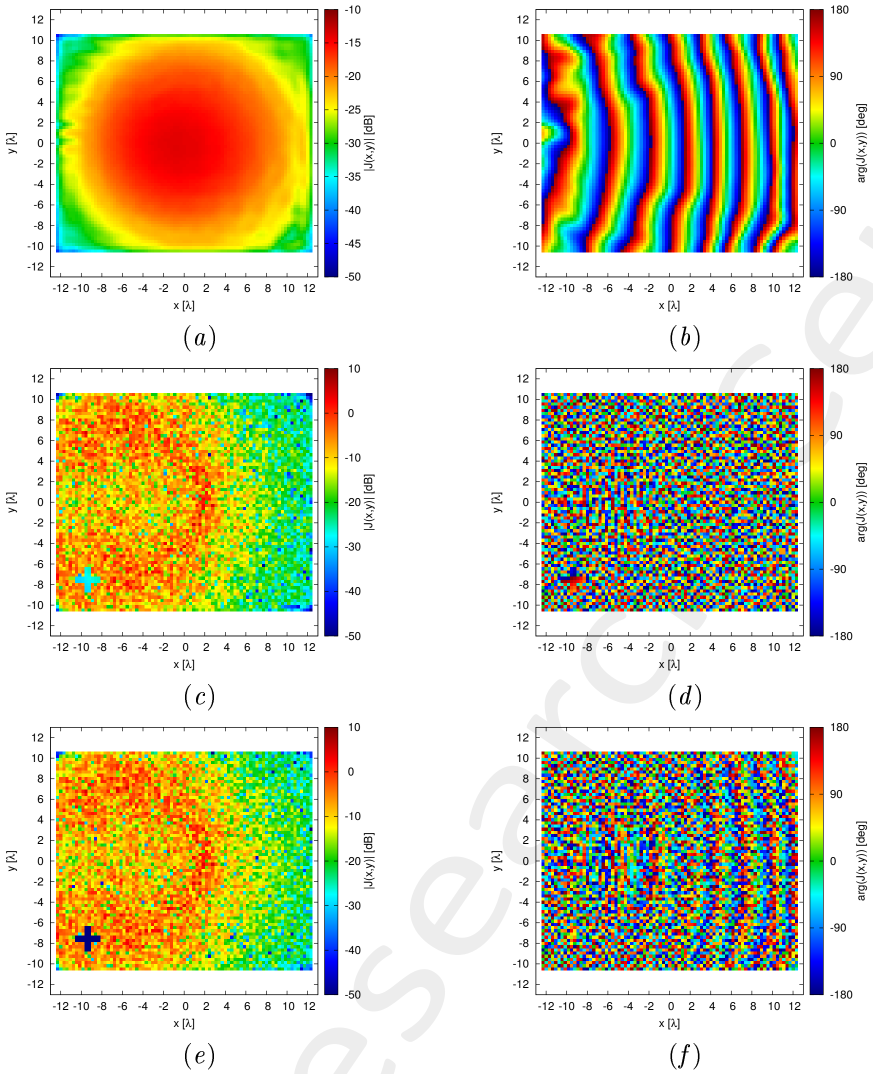

Figure 33: $(a)(c)(e)$ Magnitude and $(b)(d)(f)$ phase $(a)(b)$ of $J^{MN}(x,y)$, $(c)(d)$ $J^{NR}(x,y;\underline{\alpha})$, and $(e)(f)$ $J^{TOT}(x,y;\underline{\alpha})$.

Radiated Field

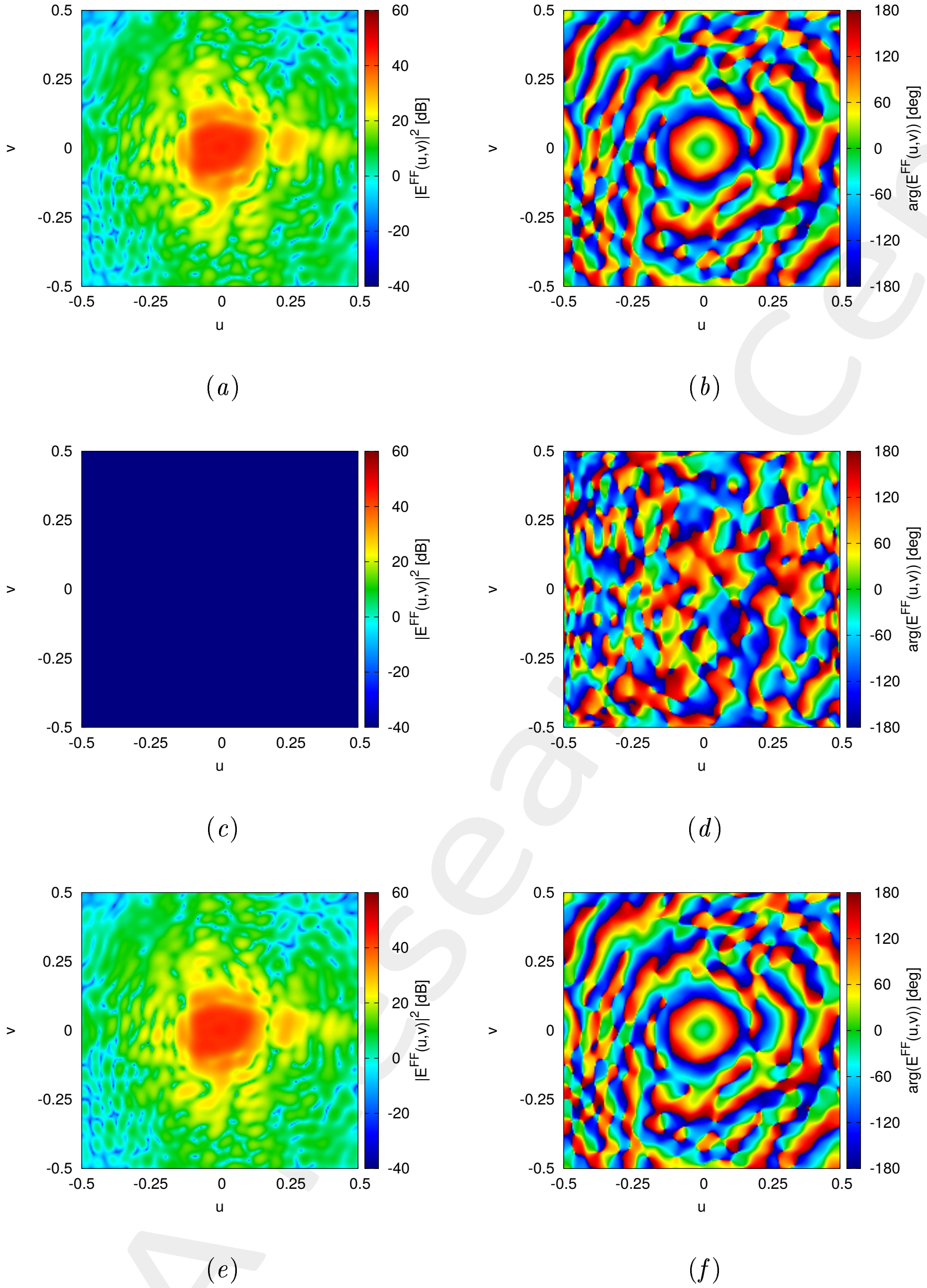

Figure 34: $(a)(c)(e)$ Magnitude and $(b)(d)(f)$ phase of the radiated field by $(a)(b)$, $J^{MN}(x,y)$, $(c)(d)$ $J^{NR}(x,y;\underline{\alpha})$, and $(e)(f)$ $J^{TOT}(x,y;\underline{\alpha})$.

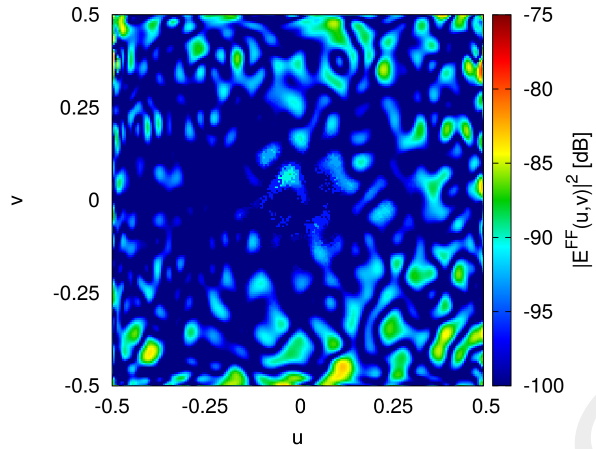

Figure 35: Magnitude of the difference between the radiated fields by $J^{MN}(x,y)$ and $J^{TOT}(x,y;\underline{\alpha})$.

References

[1] P. Rocca, G. Oliveri, R. J. Mailloux, and A. Massa, “Unconventional phased array architectures and design methodologies: A review,” *Proc. IEEE*, vol. 104, no. 3, pp. 544-560, Mar. 2016.

[2] P. Rocca, L. Poli, N. Anselmi, M. Salucci, and A. Massa, “Predicting antenna pattern degradations in microstrip reflectarrays through interval arithmetic,” *IET Microw., Antennas Propag.*, vol. 10, no. 8, pp. 817-826, Mar. 2016.

[3] M. Salucci, L. Tenuti, G. Oliveri, and A. Massa, “Efficient prediction of the EM response of reflectarray antenna elements by an advanced statistical learning method,” *IEEE Trans. Antennas Propag.*, vol. 66, no. 8, pp. 3995-4007, Aug. 2018.

[4] M. Salucci, A. Gelmini, G. Oliveri, N. Anselmi, and A. Massa, “Synthesis of shaped beam reflectarrays with constrained geometry by exploiting non-radiating surface currents,” *IEEE Trans. Antennas Propag.*, vol. 66, no. 11, pp. 5805-5817, Nov. 2018

[5] G. Oliveri, Y. Zhong, X. Chen, and A. Massa, “Multi-resolution subspace-based optimization method for inverse scattering,” *J. Opt. Soc. Amer. A*, Opt. Image Sci., vol. 28, no. 10, pp. 2057-2069, Oct. 2011.

[6] L. Poli, G. Oliveri, F. Viani, and A. Massa, “MT-BCS-based microwave imaging approach through minimum-norm current expansion,” *IEEE Trans. Antennas Propag.*, vol. 61, no. 9, pp. 4722-4732, Sep. 2013.

[7] N. Anselmi, P. Rocca, M. Salucci, and A. Massa, “Irregular phased array tiling by means of analytic schemata-driven optimization,” *IEEE Trans. Antennas Propag.*, vol. 65, no. 9, pp. 4495-4510, Sep. 2017.

[8] L. Poli, P. Rocca, M. Salucci, and A. Massa, “Reconfigurable thinning for the adaptive control of linear arrays,” *IEEE Trans. Antennas Propag.*, vol. 61, no. 10, pp. 5068-5077, Oct. 2013.

[9] L. Poli, G. Oliveri, P. Rocca, M. Salucci, and A. Massa, "Long-Distance WPT Unconventional Arrays Synthesis" *Journal of Electromagnetic Waves and Applications*, vol. 31, no. 14, pp. 1399-1420, Jul. 2017.

[10] M. Salucci, G. Gottardi, N. Anselmi, and G. Oliveri, “Planar thinned array design by hybrid analytical-stochastic optimization,” *IET Microwaves, Antennas & Propagation*, vol. 11, no. 13, pp. 1841-1845, Oct. 2017.

[11] P. Rocca, T. Moriyama, N. Anselmi, and A. Massa, “Robust prediction of the radiated pattern features with uncertainties in reflectarray design,” 2014 IEEE Antenna Conference on Antenna Measurements and Applications (IEEE CAMA 2014), Antibes Juan-les-Pins, France, pp. 1-3, November 16-19, 2014.

[12] G. Oliveri, A. Gelmini, M. Salucci, D. Bresciani, and A. Massa, “Exploiting non-radiating currents in reflectarray antenna design,” 11th European Conference on Antennas and Propagation (EUCAP 2017), Paris, France, pp. 88-91, March 19-24, 2017.